THE ASTROPHYSICAL JOURNAL, 435:909–919, 1994 November 10

ELECTRON ENERGY DEPOSITION IN CARBON MONOXIDE GAS

WEIHONG LIU AND G. A. VICTOR
Harvard-Smithsonian Center for Astrophysics, 60 Garden Street, Cambridge, MA 02138
Received 1994 March 7; accepted 1994 May 12

ABSTRACT

A comprehensive set of electron impact cross sections for carbon monoxide molecules is presented on the basis of the most recent experimental measurements and theoretical calculations. The processes by which energetic electrons lose energy in CO gas are analyzed with these input cross sections. The efficiencies are computed of vibrational and electronic excitation, dissociation, ionization, and heating for CO gas with fractional ionization ranging from 0% to 10%. The calculated mean energy per ion pair for neutral CO gas is 32.3 eV, which is in excellent agreement with the experimental value of 32.2 eV. It increases to 35.6 eV at a fractional ionization of 1%, typical of supernovae ejecta.

Subject heading: molecular processes

1. INTRODUCTION

The processes by which energetic electrons lose energy in carbon monoxide gas are important in many astrophysical objects. Electron impact excitation of CO contributes to the observed Cameron ($a\,^3\Pi \rightarrow X\,^1\Sigma^+$) and fourth positive ($A\,^1\Pi \rightarrow X\,^1\Sigma^+$) band emissions from the upper atmosphere of the planet Mars. Dissociative recombination following electron impact ionization of CO and electron impact dissociation of CO may account for the observed abundance of atomic carbon and resolve the discrepancy between models and observations of the CO/C ratio in the inner coma of comet Halley (Woods et al. 1986; Woods, Feldman, & Dymond 1987). Cravens et al. (1987) have pointed out that electron impact ionization is of comparable importance to photoionization for many molecules including CO in the magnetosheaths of comets Halley and Giacobini-Zinner. Electron impact excitation of CO is a significant source of the Cameron band emissions from comet P/Hartley 2 observed by the *Hubble Space Telescope* (Weaver et al. 1994). Production of CO^+ ions in the Venus night-side ionosphere is by both chemical transport reactions and electron impact ionization of CO (Fox & Taylor 1990). Electron impact ionization and dissociation of CO are important loss mechanisms of the CO molecules formed in the ejecta of the supernova SN 1987A (Liu, Dalgarno, & Lepp 1992).

A general study of the electron energy deposition in neutral carbon monoxide gas was carried out earlier by Sawada, Sellin, & Green (1972) based on a limited set of electron impact cross sections which they developed semiempirically. Their calculated mean energy per ion pair of 35.8 eV is significantly higher than the experimental value of 32.2 eV (Klots 1968), indicating that either the excitation cross sections have been overestimated or the ionization cross sections have been underestimated, or both.

In this paper we present a comprehensive set of electron impact cross sections of CO based mainly on the most recent experimental measurements and theoretical calculations. We apply it to study the electron energy deposition processes in CO gas with fractional ionization ranging from 0 to 10^{-1}. We provide a detailed description and calculate the efficiencies of excitation, dissociation, and ionization processes. We consider in our calculations the electron energy deposition in heat including both the energy transfer in the Coulomb collisions with ambient thermal electrons and the kinetic energy release of dissociation fragments. We recalculate the mean energy per ion pair and compare it with the experimental value. A combination of the cross sections of CO presented here with those of atomic oxygen and carbon, which are the major constituents in the ejecta of SN 1987A, will make possible a more complete analysis of the ionization, heating, cooling, and chemistry of SN 1987A.

2. CROSS SECTIONS AND LOSS FUNCTIONS

We considered in our calculations 10 excited vibrational levels of the ground electronic $X\,^1\Sigma^+$ state of CO, 11 excited electronic states of CO, $a\,^3\Pi$, $A\,^1\Pi$, $a'\,^3\Sigma^+$, $d\,^3\Delta$, $e\,^3\Sigma^-$, $I\,^1\Sigma^-$, $D\,^1\Delta$, $b\,^3\Sigma^+$, $B\,^1\Sigma^+$, $C\,^1\Sigma^+$, $E\,^1\Pi$, and five ionization states including the ground and two excited electronic states of CO^+, $X\,^2\Sigma^+$, $A\,^2\Pi_i$, and $B\,^2\Sigma^+$, and the ground electronic states of C^+ and O^+. Rotational levels were not included because energy loss due to rotational excitation is negligibly small compared with the other energy loss channels.

2.1. *Vibrational Excitation*

The cross sections for electron impact excitation of the vibrational $v = 1$ level of CO were obtained from the measurements of Sohn et al. (1985) for the direct vibrational excitation below 1 eV, and of Ehrhardt et al. (1968) from the $^2\Pi$ shape resonance region between 1 and 4 eV with a multiplying factor of 1.3 according to Haddad & Milloy (1983) from their swarm experiments. In the higher energy range of 3–100 eV the measured cross sections of Chutjian & Tanaka (1980) exhibit a broad Σ shape resonance near 20 eV for the integral cross sections but underestimate by about a factor of 2 the differential cross sections in the energy range 20–50 eV measured by Middleton, Brunger, & Teubner (1992). We adopted the cross sections reported by Chutjian & Tanaka (1980) but multiplied them by a factor of 2. The cross sections have also been investigated by Hake & Phelps (1967) and Land (1978) in swarm experiments, and the relative cross sections have been measured by Allan (1989). The direct vibrational excitation of CO

follows the $\Delta v = 1$ selection rule, so that excitation to higher vibrational levels is only possible via resonant processes. The cross sections for the excitation of the higher vibrational levels were obtained from the measurements of Ehrhardt et al. (1968) for $v = 2$–7 and of Boness & Schulz (1973) for $v = 8$–10, again multiplied by a factor of 1.3 (Haddad & Milloy 1983). The experimental results are in good agreement on the shape of the cross sections with the theoretical calculations of Sohn et al. (1985) below the resonance energy, and of Zubek & Szmytkowski (1977), Kazansky & Yelets (1984), and Morgan (1991) above the resonance energy. However, the theoretical calculations underestimate the cross sections below the resonance energy and overestimate them above by roughly 40%.

2.2. *Electronic Excitation*

There have been only fragmentary cross section data for electron impact electronic excitation of CO until recently. Early measurements of cross sections for electronic excitation of CO have mostly been limited to integral cross sections, and they have been restricted to those which may be measured by the detector of photon emission or of metastable states. Emission measurements have been carried out by Ajello (1971) for the fourth positive ($A\,^1\Pi \rightarrow X\,^1\Sigma^+$) and the Cameron ($a\,^3\Pi \rightarrow X\,^1\Sigma^+$) system, by Mumma, Stone, & Zipf (1971) for the $A\,^1\Pi \rightarrow X\,^1\Sigma^+$ transition, by Aarts & de Heer (1970) for the $A\,^1\Pi \rightarrow X\,^1\Sigma^+$, $B\,^1\Sigma^+ \rightarrow X\,^1\Sigma^+$, and $C\,^1\Sigma^+ \rightarrow X\,^1\Sigma^+$ transitions, and by Skubenich (1967) for the $b\,^3\Sigma^+$, $d\,^3\Pi$, and $B\,^1\Sigma^+$ states. The cross sections for the excitation of the $a'\,^3\Sigma^+$ state have been obtained by Land (1978) in swarm experiments. The cross sections for the excitation of the metastable $I\,^1\Sigma^-$ state have been measured by Well, Borst, & Zipf (1978) and later by Mason & Newell (1988). Recently, Middleton, Brunger, & Teubner (1993) reported the first comprehensive set of differential cross sections in the forward direction for electron impact excitation of the $a\,^3\Pi$, $a'\,^3\Sigma^+$, $d\,^3\Delta + e\,^3\Sigma^- + I\,^1\Sigma^- + D\,^1\Delta$, $A\,^1\Pi$, $b\,^3\Sigma^+$, $B\,^1\Sigma^+$, $j\,^3\Sigma^+$, and $C\,^1\Sigma^+ + c\,^3\Pi$ states. There are also recent unpublished experimental data of S. Trajmar (1992) for the differential cross sections for the excitation of the $a\,^3\Pi$, $A\,^1\Pi$, $a'\,^3\Sigma^+$, and $d\,^3\Delta$ states at 12.5 and 15 eV presented by Sun, Winstead, & McKoy (1992). Allan (1989) and Furlong & Newell (1993) have measured the relative integral cross sections for the excitation of the $a\,^3\Pi$ state. The differential cross sections for the excitation of the $B\,^1\Sigma^+$, $C\,^1\Sigma^+$, and $E\,^1\Pi$ states have been measured by Kanik, Ratliff, & Trajmar (1993a) from the energy loss spectra at 100 eV, and the integral cross sections have been obtained by integration of the differential cross sections. The cross sections for the excitation of the $B\,^1\Sigma^+$, $C\,^1\Sigma^+$, and $E\,^1\Pi$ states have also been obtained by James et al. (1992) in emission experiments in the wavelength range of 400–1250 Å at electron impact energies of 20 and 200 eV.

Theoretical studies have been reported by Chung & Lin (1974), who calculated the integral cross sections using the Born-Ochkur-Rudge approximation for electron impact excitation of a large number of electronic states of CO, including the singlet states $A\,^1\Pi$, $E\,^1\Pi$, $B\,^1\Sigma^+$, $C\,^1\Sigma^+$, and $D\,^1\Delta$ in the energy range from threshold to 1000 eV, and the triplet states of $a\,^3\Pi$, $c\,^3\Pi$, $b\,^3\Sigma^+$, $j\,^3\Sigma^+$, $a'\,^3\Sigma^+$, and $d\,^3\Delta$ in the energy range from threshold to 100 eV. Although it may work well at high energies, the Born theory is not capable of predicting resonance behavior, and the agreement between theory and experiment is generally not good at low and intermediate energies. Lee & McKoy (1992) have reported distorted-wave calculations of both differential and integral cross sections for the excitation of the $A\,^1\Pi$, $D\,^1\Delta$, $a\,^3\Pi$, $a'\,^3\Sigma^+$, and $d\,^3\Delta$ states of CO in the energy range of 20–50 eV. The distorted-wave calculations overestimate the cross sections because of the effects of shape resonances (Lee & McKoy 1983) but give qualitatively correct shapes for the differential cross sections. Weatherford & Huo (1990) have used the Schwinger multichannel variational method to calculate both the differential and integral cross sections for the excitation of the $b\,^3\Sigma^+$ state in the energy range of threshold to 20 eV, where many sharp peak structures appear due to the resonance states of CO^-. Sun et al. (1992) have recently applied the Schwinger multichannel variational method and used single configuration (SCF) wave functions to calculate the differential and integral cross sections for the electron impact excitation of the lowest seven electronically excited states of CO, including the $a\,^3\Pi$, $A\,^1\Pi$, $a'\,^3\Sigma^+$, $e\,^3\Sigma^-$, $d\,^3\Delta$, $I\,^3\Sigma^-$, and $D\,^1\Delta$ states in the energy range of threshold to 30 eV. Most recently, Morgan & Tennyson (1993) have used the R-matrix method and configuration interaction (CI) expansions to obtain the cross sections for the excitation of the same seven states in a shorter energy range from threshold to 18 eV. The cross sections obtained using the two methods agree only broadly in the magnitudes they predict, and differ in the shapes. Morgan & Tennyson (1993) utilized CI target wave functions which are better than the SCF wave functions used by Sun et al. (1992), except for the optically allowed transition to the $A\,^1\Pi$ state, for which the CI target wave function is particularly poor. Morgan & Tennyson (1993) also treated the effects of correlation and polarization better than Sun et al. (1992). However, the cross sections obtained using the R-matrix method are unreliable above 15 eV because of the unavailability of CI target wave functions for the higher excited states which couple strongly to the states of interest. The Schwinger multichannel method is much less affected by omitting target states and gets better above 15 eV, where correlation and polarization are not important. We use the cross sections based on the calculations of Sun et al. (1992), which have broader energy coverage and allow a connection to the cross sections calculated at higher energies using the Born approximation (Chung & Lin 1974). Adopting the cross sections presented by Morgan & Tennyson (1993) would result in a significant increase in the electronic excitation efficiency and a significant decrease in the ionization and heating efficiencies.

In our calculations, the cross sections for the excitation of the $a\,^3\Pi$ and $A\,^1\Pi$ states were obtained from the calculations of Sun et al. (1992) in the energy range of threshold to 30 eV, which give differential cross sections in good agreement with the experimental results of Middleton et al. (1993) and the unpublished experimental data of Trajmar. At higher energies the cross sections for the excitation of the $a\,^3\Pi$ state calculated by Chung & Lin (1974) were adopted and normalized to that calculated by Sun et al. (1992) at 30 eV. The cross sections for the excitation of the $a\,^3\Pi$ state calculated by Morgan & Tennyson (1993) have a peak with magnitude higher by 20% at an energy lower by about 1 eV, but it has a tail with lower magnitudes at higher energies. Adopting the cross sections for the excitation of the $a\,^3\Pi$ state calculated by Morgan & Tennyson (1993) would result in a small change in the energy deposition in CO gas. The cross sections for the excitation of the $A\,^1\Pi$ state calculated by Morgan & Tennyson (1993) are about twice as large as that calculated by Sun et al. (1992) and lie considerably above those measured by Ajello (1971) and Mumma et al. (1971). Morgan & Tennyson (1993) expected their cross sections for the excitation of the $A\,^1\Pi$ state to be less reliable than

those calculated by Sun et al. (1992) because of the nonconvergence with respect to the sum over symmetries and the poor CI calculated by Morgan & Tennyson (1993) would increase the mean energy per ion pair for CO gas by more than 2 eV.

The cross sections for the excitation of the $a'\,^3\Sigma^+$ state were given by the calculations of Sun et al. (1992) below 30 eV and of Lee & McKoy (1982) from 30 to 50 eV. There is a reasonable agreement in the differential cross sections for the excitation of this state between the calculations of Sun et al. (1992) and Lee & McKoy (1982) and the measurements of Middleton et al. (1993) and the unpublished experimental data of Trajmar. The cross sections of Chung & Lin (1974) at higher energies were adopted and scaled to the cross section of Lee & McKoy (1982) at 50 eV. Adopting the cross sections calculated by Morgan & Tennyson (1993), which lie below those calculated by Sun et al. (1992), would result in only a slight decrease in the mean energy per ion pair because the excitation of this state is not a dominant energy loss channel.

The calculations of Sun et al. (1992) overestimate the summed differential cross sections for the excitation of the $e\,^3\Sigma^-$, $d\,^3\Delta$, $I\,^1\Sigma^-$, and $D\,^1\Delta$ states by about an order of magnitude, compared with the measurements of Middleton et al. (1993), as do the calculations of Weatherford & Huo (1990) for the excitation of the $b\,^3\Sigma^+$ state by a factor of 5. The shapes of the theoretical and experimental differential cross sections are in good agreement. We used the cross sections calculated by Sun et al. (1992) for the excitation of the $e\,^3\Sigma^-$, $d\,^3\Delta$, and $D\,^1\Delta$ states, and by Weatherford & Huo (1900) for the excitation of the $b\,^3\Sigma^+$ state, but reduced them by factors of 10 and 5, respectively. At higher energies, the theoretical cross section of Chung & Lin (1974) for the excitation of the $d\,^3\Delta$, $D\,^1\Delta$, and $b\,^3\Sigma^+$ states were adopted and scaled to the cross sections of Sun et al. (1992) at 30 eV and of Weatherford & Huo (1990) at 20 eV, and the cross sections for the excitation of the $e\,^3\Sigma^-$ state were assumed to have typical triplet energy dependence. The cross sections for the excitation of the higher lying metastable $I\,^1\Sigma^-$ state were given by the measurements of Mason & Newell (1988) in the energy range of threshold to 60 eV, where the cross sections were normalized to the maximum value in the earlier measurements of Well et al. (1973), and the influence of the high vibrational levels on the lower lying metastable $a\,^3\Pi$ state was removed. The theoretical cross sections of Sun et al. (1992) for the excitation of the $I\,^1\Sigma^-$ state agree within the experimental uncertainty of a factor of 3 with the measured cross sections. At higher energies, the cross sections for the excitation of this state were assumed to have the same energy dependence as that for the excitation of the $D\,^1\Delta$ state. Since these two excited states are both dipole-forbidden from the ground state, the cross sections are small, and the large uncertainties in the cross sections have little effect on the energy deposition process. The cross sections for the excitation of the $e\,^3\Sigma^-$, $d\,^3\Delta$, and $D\,^1\Delta$ states calculated by Morgan & Tennyson (1993) are all significantly smaller than those calculated by Sun et al. (1992), but still their differential cross sections are expected to be substantially larger than those measured by Middleton et al. (1993), and smaller scaling factors would be necessary to normalize the cross sections calculated by Morgan & Tennyson (1993) to the measurements of Middleton et al. (1993). In any case, adopting the cross sections for the excitation of the $e\,^3\Sigma^-$, $d\,^3\Delta$, and $D\,^1\Delta$ states calculated by Morgan & Tennyson (1993) instead of those calculated by Sun et al. (1992) would have a negligible effect on the energy deposition process because these cross sections are much smaller than those for the dominant excitation channels such as the excitation of the $a\,^3\Pi$ and $A\,^1\Pi$ states.

We obtained the integral cross sections for the excitation of the $B\,^1\Sigma^+$ and $E\,^1\Pi$ states in the energy range 20–50 eV by extrapolating and integrating the differential cross sections data measured by Middleton et al. (1993) in the forward direction where they are strongly peaked. The cross sections for the excitation of the $C\,^1\Sigma^+$ state in the energy range of threshold to 100 eV were obtained from the emission measurements of James et al. (1992) and normalized to the measured cross section of Kanik et al. (1993a) at 100 eV. At higher energies the cross sections for the excitation of the $B\,^1\Sigma^+$, $C\,^1\Sigma^+$, and $E\,^1\Pi$ states were obtained by scaling the theoretical cross sections of Chung & Lin (1974) to the measured cross sections of Kanik et al. (1993a) at 100 eV. The emission cross sections of the $B\,^1\Sigma^+$, $C\,^1\Sigma^+$, and $E\,^1\Pi$ states at 200 eV measured by James et al. (1992) are in good agreement with those measured by Kanik et al. (1993a) from energy loss spectra at 100 eV. However, the emission cross section of the $B\,^1\Sigma^+$ state at 20 eV is significantly larger than the integrated differential cross section measured by Middleton et al. (1993), possibly due to coupling of close-lying triplet states at low energies (James et al. 1992).

Most of the excited states with energy threshold above the dissociation limit of 11.092 eV and below the first ionization potential of 14.01 eV predominantly dissociate (Viala et al. 1988). We assumed their dissociation probabilities to be 100%, and their effects on the electron energy degradation were accounted for by the dissociation processes discussed below. The exceptions are the $C\,^1\Sigma^+$ state, which predominantly radiates, and the $E\,^1\Pi$ state, whose dissociation probability is about 90% (Viala et al. 1988; Cosby 1993). We assumed that the $C\,^1\Sigma^+$ state does not predissociate, and we reduced by a factor of 10 the excitation yield for the $E\,^1\Pi$ state. The electron energy loss due to the excitation of the states with threshold above the first ionization threshold was accounted for by the ionization processes discussed below because these states predominantly autoionize.

2.3. *Dissociation*

Measurements of electron impact dissociation cross sections of CO had been restricted to emission measurements of dissociative excitation of CO (Ajello 1971; Aarts & de Heer 1970; James et al. 1992). Cosby (1993) has recently measured in a crossed-beam experiment the total electron impact dissociation cross sections of CO, exclusive of dissociative ionization contributions, at electron energies between the dissociation limit and 200 eV. He found that dissociation of CO is predominantly via predissociating states between the dissociation threshold of 11.09 eV and the first ionization potential of 14.01 eV, and that the dissociated fragments are predominantly the ground-state products $C(^3P)$ and $O(^3P)$. No significant continuum dissociation was observed (Cosby 1993), nor was it expected by theory, because no repulsive states exist in this energy region (Cooper & Kirby 1987; Kirby & Cooper 1989). We adopted the cross sections measured by Cosby (1993) and extrapolated them to higher energies by assuming the dissociation of CO at high energies to be due mainly to the optically allowed predissociating states of CO. Based on the kinetic energy release spectrum of the dissociation products of CO measured by Cosby (1993), we treated the dissociation of CO as a discrete process and assumed an average electron energy loss of 12.94 eV per dissociation of CO, of which 1.85 eV

appears as the kinetic energy of the dissociation products and inputs as heat.

2.4. *Ionization*

The electron impact ionization cross sections of CO for the production of CO^+ have been measured by Rapp & Englander-Golden (1965), Hille & Märk (1978), Orient & Srivastava (1987), and Freund, Wetzel, & Shul (1990), and they are in agreement within the combined experimental uncertainties. Ajello (1971) has reported the emission cross sections of the comet tail system ($A\,^2\Pi \rightarrow X\,^2\Sigma^+$) and the first negative band system ($B\,^2\Sigma^+ \rightarrow X\,^2\Sigma^+$) of CO^+ following electron impact of CO. Orient & Srivastava (1987) have also measured the dissociative ionization cross sections for the production of C^+ and O^+. There also exist semiempirical calculations of the total ionization cross sections of CO by Jain & Khare (1976), which agree with the experimental results within the experimental uncertainties.

We adopted the electron impact ionization cross sections of Ajello (1971) for the production of the excited $A\,^2\Pi_i$ and $B\,^2\Sigma^+$ states of CO^+, and the total parent ionization cross sections of CO of Orient & Srivastava (1987), from which the cross sections for the production of the ground $X\,^2\Sigma^+$ state of CO^+ were obtained by subtracting the cross sections for the production of the $A\,^2\Pi$ and $B\,^2\Sigma^+$ states. We also adopted the dissociative ionization cross sections of Orient & Srivastava (1987) for the production of the C^+ and O^+ fragment ions. Because of the lack of knowledge of the distribution of the kinetic energy produced in the dissociative ionization process of CO, we assumed that all the kinetic energy is carried by the electrons. The uncertainty of the heating efficiency caused by this assumption is small even for low fractional ionizations because of the relatively low dissociative ionization cross sections. We ignored in our calculations the double ionization of CO by electron impact because it accounts for less than 1% of total ionization (Hille & Märk 1978).

Ionizations by the primary electrons create secondary electrons, and they contribute effectively to excitation, dissociation, ionization, and heating of CO gas. The differential cross sections of ionization for the production of a secondary electron of energy E_s by impact of a primary electron of energy E_p have been measured by Opal, Peterson, & Beaty (1971). It may be written

$$\frac{d\sigma^i(E_p, E_s)}{dE_s} = \frac{C(E_p)}{1 + (E_s/\bar{E})^{2.1}}, \tag{1}$$

where $C(E_p)$ is a normalization factor which may be determined by equating the numerical integral of the differential cross sections to the integral cross sections of ionization, and $\bar{E}$ is a shape parameter which is 14.2 eV for CO.

2.5. *Heating Rate*

Energy loss rate to heating the ambient thermal electrons of density n_e and temperature T_e was included in our calculations using the analytical fit of Swartz, Nisbet, & Green (1971), which gives a convenient representation of the loss function formulae of Itikawa & Aono (1966) and Schunk & Hays (1971). It may be written

$$\frac{dE}{dt} = -\frac{2.00 \times 10^{-4} n_e^{0.97}}{E^{0.44}} \left(\frac{E - T_e}{E - 0.53T_e}\right)^{2.36}. \tag{2}$$

This rate is insensitive to the electron temperature for temperatures of the order of 1000 K. We chose a temperature of 2000 K appropriate for the ejecta of SN 1987A. In comparison, energy loss in elastic scattering of CO is negligible, and it was not included in the heat input.

2.6. *Total Cross Sections*

The references for all the cross sections used in our calculations are listed in Table 1. The cross sections for the vibrational excitation, electronic excitation to the triplet states, electronic excitation to the singlet states and dissociation, and ionization are presented in Figures 1*a*, 1*b*, 1*c*, and 1*d*, respectively. The total cross sections for the vibrational excitation, electronic excitation and dissociation, and ionization are shown in Figure 2. For comparison, the recommended total cross sections of Kanik, Trajmar, & Nickel (1993b) are plotted in the same figure. Their recommended total vibrational excitation cross sections are from the measurements of Ehrhardt et al. (1968) and Chutjian & Tanaka (1980). However, Kanik et al. (1993b) included only the $v = 0 \rightarrow 1$ transition and neglected a large contribution from excitation to the higher vibrational levels. Our total cross sections for the vibrational excitation are significantly larger than those recommended by Kanik et al. (1993b), owing to the neglect in the recommended cross sections of the contribution from exciting the higher vibrational levels. The recommended total ionization cross sections are those from the measurements of Rapp & Englander-Golden (1965). Our total ionization cross sections are lower, but agree with the recommended values within the experimental uncertainties. The recommended total electronic excitation cross sections were deduced from the difference between the total electron scattering cross sections and the sum of the integral cross sections for the elastic scattering, vibrational excitation, and ionization at each electron energy. There is good agreement between our total electronic excitation cross sections and the recommended values at energies below 12 eV, where excitation to the $a\,^3\Pi$ state dominates, suggesting that both the magnitude and the shape of our cross sections for this state are reasonable at these low energies. Our total electronic excitation and dissociation cross sections at high energies lie above those recommended values. This is the direct result of our ionization cross sections being lower than those recommended values at high energies. There would be excellent agreement at high energies if our total ionization cross sections rather than the recommended total values were subtracted in deducing the total excitation cross sections by Kanik et al. (1993b). Our total excitation and dissociation cross sections are only about half of the recommended values in the energy range 15–150 eV. This discrepancy might be partly caused by the absence in our cross section data set of contributions from excitations to high-lying Rydberg states. However, the contribution from these high-lying Rydberg states may be small, and if we adopted the recommended cross sections of Kanik et al. (1993b), the calculated mean energy per ion pair would be increased to 35.6 eV for neutral CO gas, a value considerably larger than the experimental value of 32.2 eV (Klots 1968). This discrepancy is more likely caused by the method used by Kanik et al. (1993b) in obtaining the total electronic excitation cross sections. The recommended total excitation cross sections were derived by subtracting the measured cross sections for the elastic scattering, ionization, and vibrational excitation from the measured total cross sections. Accuracies of the measured total and ionization cross sections are a few percent and at most 10%, respectively. The elastic scattering cross sections

TABLE 1

REFERENCES FOR CROSS SECTIONS OF CO

STATE	VERTICAL EXCITATION ENERGY (eV)	REFERENCES	
		Measurements	Calculations
Vibrational Excitation			
$v = 1$	0.266 (le Floch 1991)	Sohn et al. 1985 Ehrhardt et al. 1968 Haddad & Milloy 1983 Chutjian & Tanaka 1980	
$2 \le v \le 7$	0.528–1.791 (le Floch 1991)	Ehrhardt et al. 1968	
$8 \le v \le 10$	2.0–2.4 (le Floch 1991)	Boness & Schulz 1973	
Electronic Excitation			
$a\,^3\Pi$	6.32 (Tilford & Simmons (1972)	Middleton et al. 1993	Sun et al. 1992 Chung & Lin 1974
$A\,^1\Pi$	8.50 (Tilford & Simmons 1972)	Middleton et al. 1993	Sun et al. 1992 Chung & Lin 1974
$a'\,^3\Sigma^+$	8.58 (Tilford & Simmons 1972)	Middleton et al. 1993	Sun et al. 1992 Lee & McKoy 1982 Chung & Lin 1974
$d^3\Delta$	9.34 (Tilford & Simmons 1972)	Middleton et al. 1993	Sun et al. 1992 Chung & Lin 1974
$e\,^3\Sigma^-$	9.86 (Tilford & Simmons 1972)	Middleton et al. 1993	Sun et al. 1992
$I\,^1\Sigma^-$	9.45 (Mason & Newell 1988)	Mason & Newell 1988	Sun et al. 1992
$D\,^1\Delta$	9.55 (Mason & Newell 1988)	Middleton et al. 1993	Sun et al. 1992 Chung & Lin 1974
$b\,^3\Sigma^+$	10.394 (Ransil 1960)	Middleton et al. 1993	Weatherford & Huo 1990 Chung & Lin 1974
$B\,^1\Sigma^+$	10.776 (Tilford & Simmons 1972)	Middleton et al. 1993 Kanik et al. 1993a	Chung & Lin 1974
$C\,^1\Sigma^+$	11.396 (Tilford & Simmons 1972)	James et al. 1992 Kanik et al. 1993a	Chung & Lin 1974
$E\,^1\Pi$	11.522 (Tilford & Simmons 1972)	Middleton et al. 1993 Kanik et al. 1993a	Chung & Lin 1974
Dissociation			
C + O	11.09	Cosby 1993	
Ionization			
Parent CO^+	...	Orient & Srivastava 1987	
$CO^+(X\,^2\Sigma^+)$	14.01 (Potts & Williams 1974)	Ajello 1971	
$CO^+(A\,^2\Pi_i)$	16.91 (Potts & Williams 1974)	Ajello 1971	
$CO^+(B\,^2\Sigma^+)$	19.69 (Potts & Williams 1974)	Ajello 1971	
Fragment C^+	22.39	Orient & Srivastava 1987	
Fragment O^+	24.69	Orient & Srivastava 1987	

are not readily available and have been obtained from differential scattering experiments over limited angular range by extrapolating and integrating the measured values, and the accuracies can be as low as 20%. Because the total and elastic scattering cross sections are large with large absolute errors, the total excitation cross section recommended by Kanik et al. (1993b) resulting from the subtraction would have much larger relative errors and be much less accurate than our total excitation cross sections which have been determined from direct experimental measurements. It is shown in Figure 2 that the discrepancy is more serious in the low-energy region between 20 and 100 eV than in the high-energy region above 100 eV because the total and elastic scattering cross sections are larger at lower energies.

2.7. *Energy Loss Functions*

The electron energy deposition in CO gas can be characterized by the total energy loss function $L(E)$, which is the sum of the products of the cross sections and the associated energy losses for all the energy loss channels, and is expressed as

$$L(E) = \sum_n \sigma_n(E) W_n + \sum_n \int_0^{(E-I_n)/2} (I_n + E_s) \frac{d\sigma_n^i(E, E_s)}{dE_s} dE_s , \tag{3}$$

where $\sigma_n(E)$ are the excitation cross sections with the associated energy losses W_n, $d\sigma_n^i(E, E_s)/dE_s$ are the differential cross sections of ionization, and I_n and E_s are the ionization potentials and the energies of secondary electrons, respectively. From equations (1) and (3), the energy loss function can be rewritten as

$$L(E) = \sum_n \sigma_n(E) W_n + \sum_n \sigma_n^i(E) I_n \times \int_0^{(E-I_n)/(2\bar{E})} \left(1 + \frac{\bar{E}}{I_n} x\right) \frac{dx}{1 + x^{2.1}} \Big/ \int_0^{(E-I_n)/(2\bar{E})} \frac{dx}{1 + x^{2.1}} , \tag{4}$$

where $\sigma_n^i(E)$ are the integral cross sections of ionization.

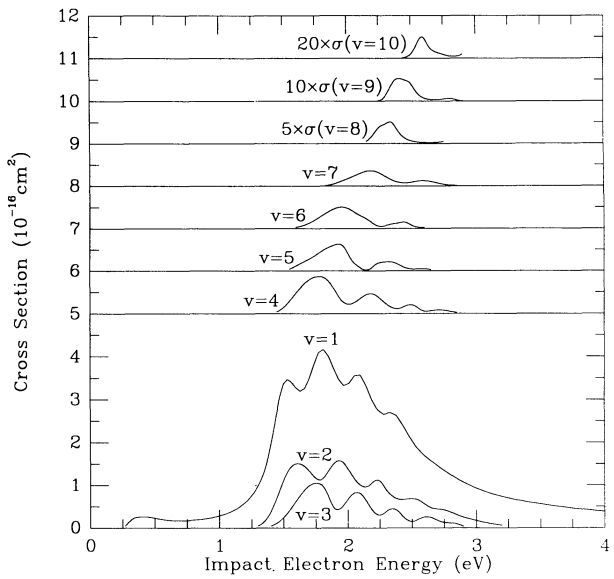

FIG. 1*a*

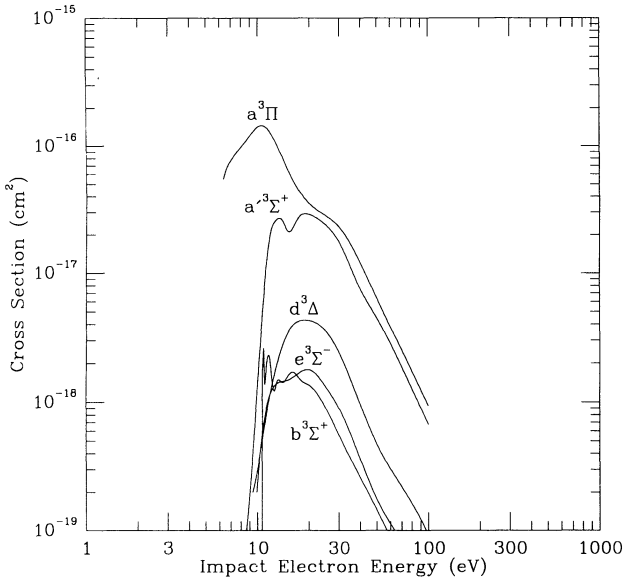

FIG. 1*b*

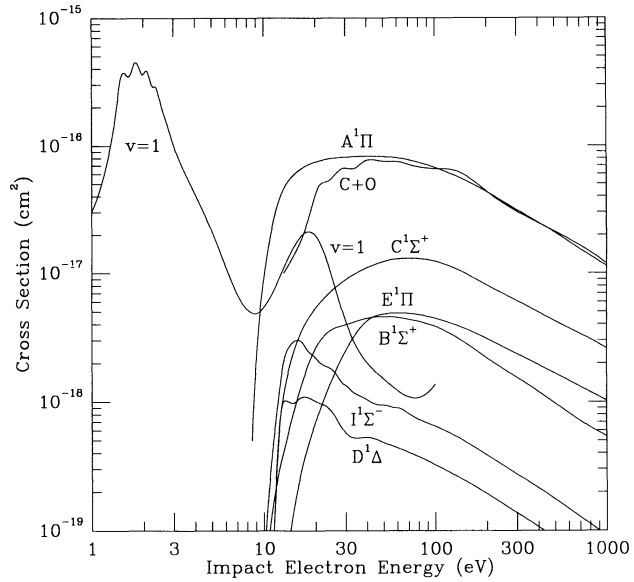

FIG. 1*c*

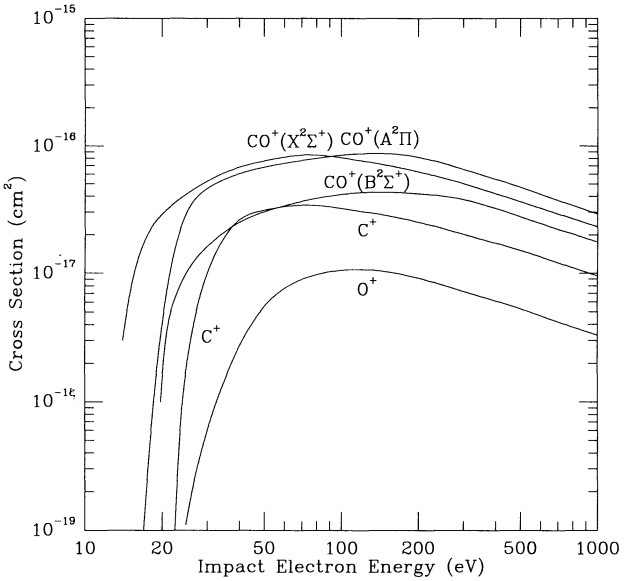

FIG. 1*d*

FIG. 1.—Electron impact cross sections of CO as a function of the impact electron energy for (*a*) the vibrational levels of the electronic ground state, (*b*) the electronically excited triplet states, (*c*) the electronically excited singlet states, and (*d*) the ionization states.

The energy loss in CO gas is dominated at high energies by ionization, in the intermediate energy range 6–28 eV by electronic excitation, and at lower energies by vibrational excitation, as shown in Figure 3. The energy loss due to dissociation is comparable to that due to the nondissociating excitation at energies higher than 40 eV, but it is lower below 40 eV, and it is much smaller than the contribution of the ionization at all energies. Our calculated total energy loss function, which peaks at 133 eV with a value of 9.34×10^{-15} cm^2 eV, is lower than that calculated by Sawada et al. (1972), which is 1.1×10^{-4} cm^2 eV at the maximum. This occurs mainly because the total excitation cross sections of Sawada et al. (1972) are considerably larger than ours. If we adopted the total excitation cross sections of Kanik et al. (1993b), the calculated total energy loss function would be increased to 9.77×10^{-15} cm^2 eV but still smaller than that of Sawada et al. (1972). The total energy loss function for CO has a value lower than but closer to that for the isoelectric molecule N_2, which is about 1.1×10^{-14} cm^2 eV at maximum (Fox & Victor 1988).

3. COMPUTATIONAL METHOD

We present here a brief description of our computational method for electron energy deposition in an ionized gas. It has been applied previously to studies of electron energy deposition in atomic oxygen (Dalgarno & Lejeune 1971), molecular hydrogen (Cravens, Victor, & Dalgarno 1975), argon (Fox, Dalgarno, & Victor 1977), carbon dioxide (Fox & Dalgarno 1979), and molecular nitrogen (Fox & Victor 1988). For a given energy E_p of primary electrons a discrete set of energies E_1, E_2, ..., E_p is selected such that the energy bin sizes $\Delta E_i =$

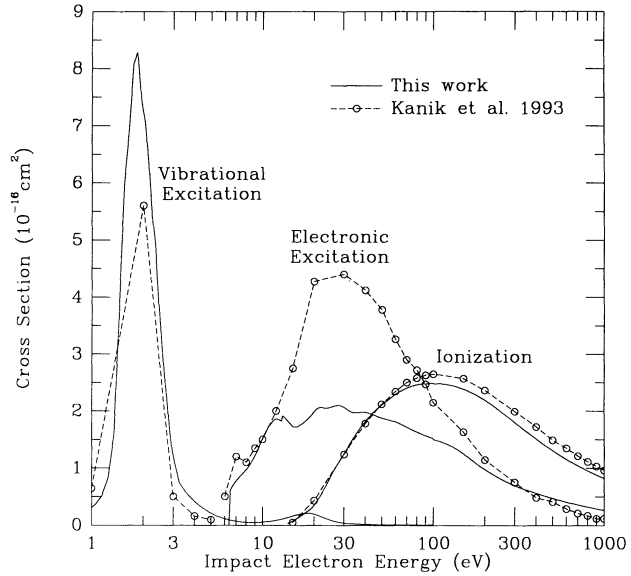

FIG. 2.—Total cross sections of CO for vibrational and electronic excitation and ionization in comparison with those recommended by Kanik et al. (1993b).

$E_i - E_{i-1}$ are smaller than the threshold energies of all the inelastic processes that contribute significantly to the energy loss at E_i. We considered in our calculations the energy deposition by 1 keV primary electrons which is appropriate for supernovae ejecta. Adopting other high energies would have a negligible effect on the energy loss efficiencies because all the energy loss channels have the same high-energy dependence. For CO gas, we chose a bin size of 0.1 eV, lower than the vibrational excitation threshold of CO of 0.266 eV, for energies lower than 100 eV where vibrational excitation to the $v = 1$ level is significant. For higher energies a larger bin size of 1 eV was chosen, lower than the electronic excitation threshold of CO of 6.01 eV. The probabilities that the bin at the highest energy is emptied by excitation, dissociation, ionization, and elastic process are computed from the electron impact cross sections and Coulomb collision rate. The effects on the overall energy degradation of superelastic collisions and radiative and dissociative attachments are small and are ignored in our calculations. Each successive lower energy bin is emptied in turn until no inelastic process is possible and all of the remaining energy inputs as heat. The rate is recorded at which each excited or ionized state of CO is populated. The total population of each excited or ionized state is the sum of the excitation or ionization yield in each step, from which the efficiencies of the excitation, dissociation, ionization, and heating can be obtained. The equilibrium flux of electrons may be derived by dividing the rate of production of electrons in each bin by the rate of loss out of the bin. The accuracy of the computational method is limited by the bin sizes chosen. For the bin sizes of 0.1 and 1 eV for energies below and above 100 eV, respectively, the uncertainty is less than 0.5%, which is much smaller than the uncertainties of at least 10% for the input cross sections of CO.

4. MEAN ENERGY PER ION PAIR

The mean energy per ion pair, defined as the energy of primary electrons divided by the number of ion pairs produced, is shown in Figure 4 as a function of fractional ionization of CO gas from $X_e = 10^{-6}$ to $X_e = 10^{-1}$. For neutral CO gas, the calculated mean energy per ion pair is 32.3 eV, compared with the experimental value of 32.2 eV (Klots 1968). The good agreement between our calculations and the measurements indicates a reasonable accuracy for the electron impact cross sections used in our calculations for the dominant energy loss channels in CO, which include the excitation of the $a\,^3\Pi$ state in the energy range 6–15 eV, and at higher energies the excitation of the $A\,^1\Pi$ state, dissociation, and ionization. The effects on the calculated mean energy per ion pair of the uncertainties of the cross sections for nondominant processes are small. The

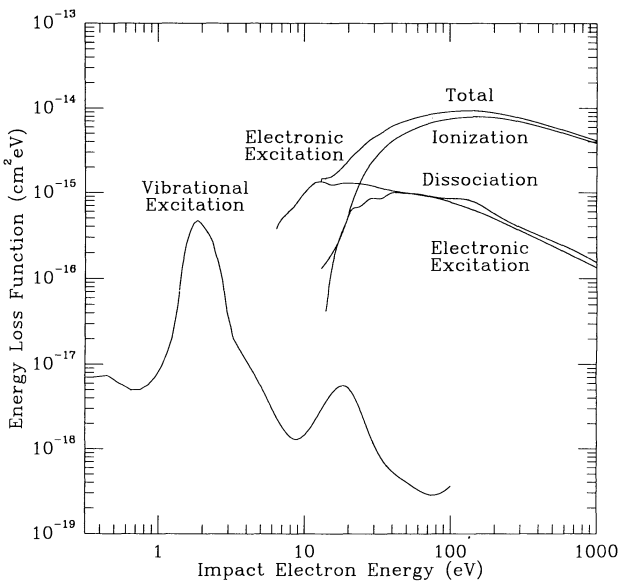

FIG. 3.—Electron energy loss function $L(E)$ for CO as a function of the impact electron energy. The individual contributions arising from vibrational and electronic excitation, dissociation, and ionization are shown.

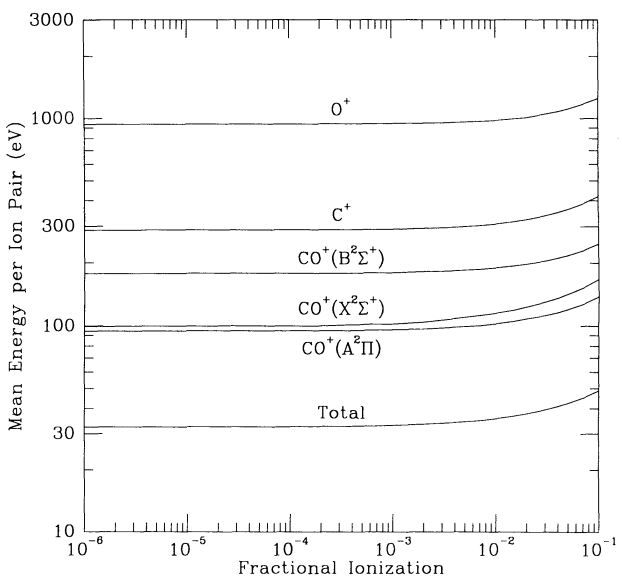

FIG. 4.—Mean energy per ion pair for CO as a function of the fractional ionization. The distributions are shown among final ion states $X\,^2\Sigma^+$, $A\,^2\Pi$, $B\,^2\Sigma^+$ of CO^+, and C^+ and O^+.

mean energy per ion pair increases with increasing fractional ionization as the Coulomb collisions absorb more of the energy of the electrons, although it is insensitive to the fractional ionization at low fractional ionizations. It increases to 33.0 eV at $X_e = 10^{-3}$, to 35.6 eV at $X_e = 10^{-2}$, and to 48.8 eV at $X_e = 10^{-1}$. The mean energy per ion pair has been previously calculated by Sawada et al. (1972) for neutral CO gas to be 35.8 eV, which is higher than ours by 3.5 eV and higher than the experimental value by 3.6 eV. An important cause of this discrepancy is that Sawada et al. (1972) greatly overestimated at high energies the cross sections for the excitation of the $a\,^3\Pi$, $C\,^1\Sigma^+$, and $E\,^1\Pi$ states, which are substantial fractions of the total excitation cross sections.

Figure 4 also shows the distribution of the ions in five different final ion states, including the ground $X\,^2\Sigma^+$ state and excited $A\,^2\Pi$ and $B\,^2\Sigma^+$ states of CO^+ and C^+ and O^+. The mean energy per ionization for each final ion state shows approximately the same dependence on fractional ionization because the ionization cross sections have a similar energy dependence. For neutral CO gas the mean energies per ionization terminating in the $X\,^2\Sigma^+$, $A\,^2\Pi$, and $B\,^2\Sigma^+$ states of CO^+ are 98.8, 93.7, and 176 eV, respectively, and the electron energy deposition efficiencies are 14.1%, 18.0%, and 11.1%, respectively. At $X_e = 10^{-2}$ the mean energies increase to 115, 102, and 189 eV, and the efficiencies decrease to 12.2%, 16.6%, and 10.6%, respectively. In dissociative ionization the mean energies are larger and the efficiencies are smaller than those for the parent ionization. The mean energies producing C^+ and O^+ ions increase from 287 and 934 eV, respectively, for neutral CO gas to 308 and 979 eV, respectively, at $X_e = 10^{-2}$, and the efficiencies decrease from 7.80% and 2.64% for neutral CO gas to 7.27% and 2.52% at $X_e = 10^{-2}$.

5. EFFICIENCY OF EXCITATION

In Figure 5 we present the electron impact excitation efficiencies of CO by showing the mean energy per excitation, defined as the energy of primary electrons divided by the number of excitations produced, for all the electronic states. The overall characteristic feature of the mean energies per excitation is that they are insensitive to the fractional ionization at low fractional ionizations for all the states. There are characteristic differences between the triplet, optically allowed singlet, and metastable singlet states in the dependence on the fractional ionization at intermediate fractional ionizations. The mean energies per excitation increase more rapidly with increasing fractional ionization for the triplet states than for the singlet states. In addition, the mean energies per excitation for the metastable $I\,^1\Sigma^-$ and $D\,^1\Delta$ states exhibit a slower increase with respect to the increasing fractional ionization than those for the triplet states, but a faster increase than those for the optically allowed singlet states. This is caused by the different shapes of the excitation cross sections between the triplet and singlet states. The cross sections for the triplet states show characteristics of singlet-to-triplet excitation, including a rapid rise in the threshold region, a narrow peak structure at energies between 10 and 20 eV, and a fast decline at higher energies. The cross sections for all the singlet states except the metastable $I\,^1\Sigma^-$ and $D\,^1\Delta$ states rise to a broad maximum at energies between 40 and 70 eV and then decrease slowly with increasing electron energy at higher energies. The cross sections for the metastable $I\,^1\Sigma^-$ and $D\,^1\Delta$ states increase rapidly in the threshold region and reach a peak at energies between 10 and 20 eV, similar to the excitation functions of the triplet states, but decrease rather slowly with increasing electron energy at higher energies, similar to that of the optically allowed singlet states. As a result, the excitation efficiencies at intermediate fractional ionizations are the most sensitive to the fractional ionization for the triplet states, moderately sensitive for the metastable singlet states, and less sensitive for the optically allowed singlet states.

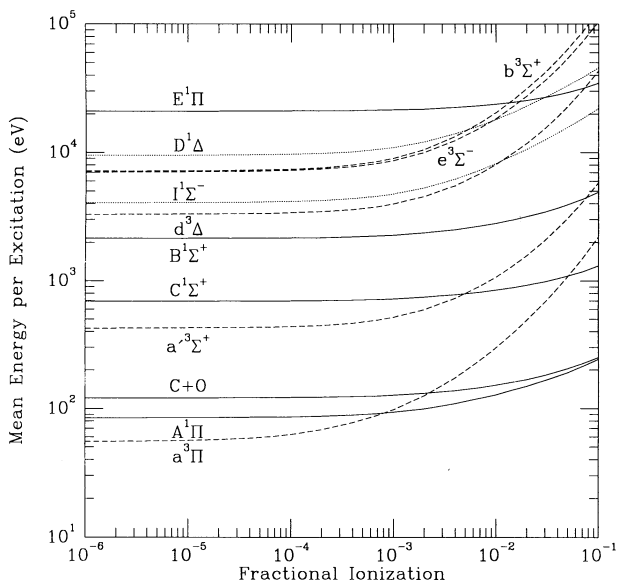

FIG. 5.—Mean energy per electronic excitation for CO as a function of the fractional ionization. The optically allowed singlet states are represented by full curves, the metastable singlet states by dotted curves, and the triplet states by dashed curves.

The electron energy loss to the electronic excitation of CO is dominated at low fractional ionizations by the excitation of the $a\,^3\Pi$ state which produces the Cameron band emissions and at high fractional ionizations by the excitation of the $A\,^1\Pi$ state which produces the fourth positive band emissions. For neutral CO the mean energies per excitation are 55.0 and 84.4 eV for the $a\,^3\Pi$ and $A\,^1\Pi$ states, respectively. The electron energy deposition efficiencies are correspondingly 11.5% and 10.1%. In comparison, Sawada et al. (1972) reported at the high-energy limit about 10% and 9% of the energy deposited in the excitation of the $a\,^3\Pi$ and $A\,^1\Pi$ states, respectively. Their values of efficiencies for the Cameron and fourth positive system are slightly smaller than ours because of the smaller excitation cross sections adopted by Sawada et al. (1972) for these states. Since the cross sections for the $a\,^3\Pi$ state have a narrower peak at lower energy than those for the $A\,^1\Pi$ state, increasing the electron abundance reduces the electron energy loss to the excitation of the $a\,^3\Pi$ state more than the excitation of the $A\,^1\Pi$ state. The mean energy per excitation increases by a factor of more than 4 to 297 eV at $X_e = 10^{-2}$ for the $a\,^3\Pi$ state, and by only a factor of 1.5 to 128 eV for the $A\,^1\Pi$ state. The associated electron energy deposition efficiencies decrease to 2.13% and 6.64%. Excitation to all the other states accounts for only about 5% of the total energy loss for neutral CO gas, and it decreases to 3% at $X_e = 10^{-2}$. Only 5.1% of the total energy loss for neutral CO gas is accounted for by the excitation of all the other electronic states, among which excitation of the $a'\,^3\Sigma^+$ and $C\,^1\Sigma^+$ states contributes most with 2.0% and 1.7%, respectively. Sawada et al. (1972) did not include the

$a'\,^3\Sigma^+$ state. They reported a higher efficiency of about 3% for the $C\,^1\Sigma^+$ state due to their larger cross sections for this state. At $X_e = 10^{-2}$ the excitation efficiencies for all the other electronic states, and the $a'\,^3\Sigma^+$ and $C\,^1\Sigma^+$ states, decrease to 3.0%, 0.8%, and 1.4%, respectively.

The mean energies per excitation with which the vibrational levels $v = 1$–10 of the ground state of CO are populated by impact of energetic electrons in CO gas are shown in Figure 6. Because of the low-energy thresholds and peaks of the cross sections, the mean energies per excitation for all these vibrational levels are the most sensitive to the fractional ionization. As the fractional ionization increases, the mean energy per excitation for the $v = 1$ level increases greatly from 4.53 eV for neutral CO gas to 641 eV for $X_e = 10^{-2}$, and the vibrational efficiency for this level decreases quickly from 5.87% to 4.15×10^{-4}. Similar behavior is found for the higher vibrational levels, except at fractional ionizations below 10^{-5} where the mean energy per excitation for the $v = 1$ level still decreases significantly with decreasing fractional ionization, while those for the higher vibrational levels are insensitive to the fractional ionization. This difference is caused by the fact that the transition $v = 0 \rightarrow 1$ is dipole-allowed and the cross sections are significant in the threshold region, while the transitions to the higher level are only possible via resonant processes and the cross sections are negligible in the threshold region.

6. EFFICIENCY OF DISSOCIATION

In Figure 5 we present the mean energy per dissociation of CO, defined as the energy of primary electrons divided by the number of dissociations of CO. The mean energy per dissociation has a dependence on the fractional ionization similar to those of the mean energies per excitation for the optically allowed singlet states because their cross sections have a similar energy dependence. The dissociation of CO is an important energy loss channel. For neutral CO gas the mean energy per dissociation is 121 eV, with an electron energy deposition efficiency of 9.2%. In comparison, Sawada et al. (1972) reported that at the high-energy limit about 5.4% of the energy is deposited in the excitation of the 13.5 eV state designated by them. This composite state may relate to the high-lying predissociating states of CO. At $X_e = 10^{-2}$ the mean energy per dissociation increases by a factor of 1.25 to 152 eV, with the associated electron energy deposition efficiencies decreasing to 7.30%.

7. ENERGY DEPOSITION AND HEATING

In Figure 7 we present the distribution of energy deposition among excitation, dissociation, ionization, and heating of CO as a function of fractional ionization from 10^{-6} to 10^{-1}. The heating efficiency includes contributions from both the Coulomb collisions and the kinetic energy release of dissociated atomic fragments. The energy deposition efficiencies of the excitation, dissociation, and ionization decrease while the heating efficiency increases with increasing fractional ionization, due to the higher Coulomb collision rates at higher fractional ionizations. More than half the electron energy loss is deposited in ionization at fractional ionizations below 10^{-2}. At fractional ionizations above 4×10^{-2}, heating is the dominant channel of energy loss by energetic electrons. The vibrational and electronic excitations, dissociation, and heating account for about 8%, 27%, 9%, and 2%, respectively, of the total electron energy loss for neutral CO gas. The total energy deposition efficiency of the electronic excitation and dissociation is about 36%, compared with the ionization efficiency of about 54%. As the fractional ionization increases, the energy deposition efficiencies of the excitation, dissociation, and ionization channels decline. The decline in the vibrational excitation efficiency is the most rapid because the vibrational excitation cross sections peak at a low energy of about 2 eV and are the most sensitive to the electron abundance. With the peaks of the cross sections for the electronic excitation and dissociation at higher energies of about 12 and 40 eV, respectively, the energy deposition efficiencies in the electronic excitation and dissociation decrease more slowly. The ionization cross sections

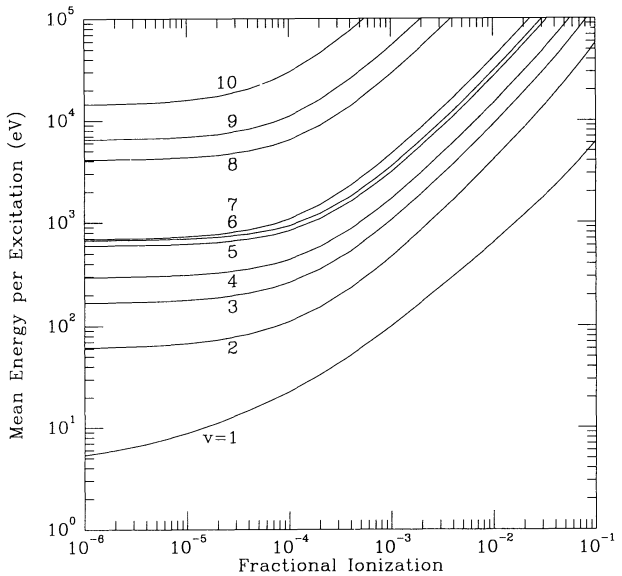

FIG. 6.—Mean energy per vibrational excitation for CO as a function of the fractional ionization.

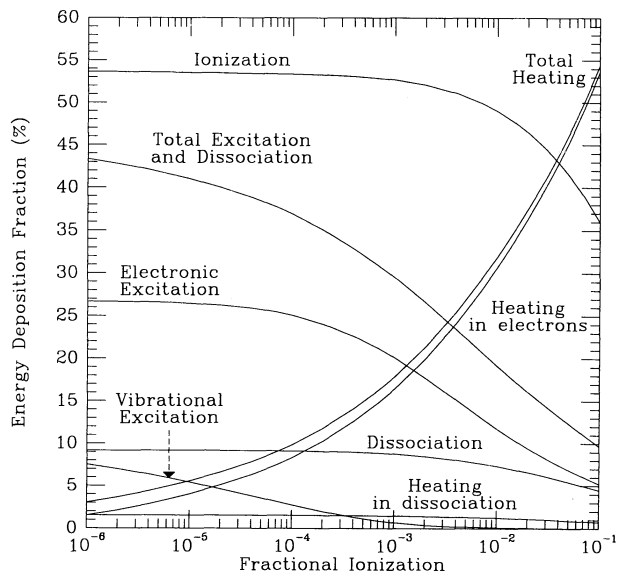

FIG. 7.—Fractions of energy deposition in excitation, dissociation, ionization, and heating for CO as a function of the fractional ionization. The heating includes contributions from Coulomb collisions with the ambient thermal electrons and from dissociation.

peak at a high energy of about 100 eV, so that there is a rather flat distribution of the ionization efficiency at fractional ionizations below 10^{-2}. At a fractional ionization of 10^{-2}, the energy deposition efficiencies of the vibrational and electronic excitations, dissociation, and ionization drop to 0.09%, 12%, 7%, and 49%, respectively, and the heating efficiency rises to 32%.

Our results for neutral CO gas can be compared with those calculated by Sawada et al. (1972) for high impact energies. Their values of the efficiencies of the electronic excitation and ionization are about equally 46%, compared with our values of 36% and 54%, respectively. The discrepancy occurs mainly because Sawada et al. (1972) overestimated the excitation cross sections. Their value for the vibrational efficiency is about 8%, which agrees with our value. Even for neutral CO gas, there is energy loss due to momentum transfer in elastic collisions and in the form of the kinetic energy release of the dissociated atomic fragments which is converted into the heat. Our calculated heating efficiency for neutral CO gas is about 2%, while Sawada et al. (1972) did not give an estimate.

In Figure 7 we also present the efficiencies for the two major heating sources of CO gas. For CO gas, a significant contribution to the heating comes from the kinetic energy release of the dissociation fragments of CO. For weakly ionized CO gas, it accounts for 1.5% of the energy deposition, comparable to the contribution from the Coulomb collisions with the ambient thermal electrons, and the total heat input is sensitive to the assumptions about the dissociation process leading to the ground-state products. As the fractional ionization increases, the total heating efficiency is less sensitive to the assumption because heating via the dissociation channel is less important and its efficiency decreases slightly due to the decrease of the dissociation efficiency. With increasing fractional ionization, an overwhelmingly larger fraction of the energy which is deposited as the heat is taken up in Coulomb collisions, and it accounts for 96% of the total heat input at $X_e = 10^{-2}$. The heated electrons transfer some of the kinetic energy to the neutral particles in elastic collisions, but most of it is lost to the vibrational excitation, which may radiate and cool the gas or undergo collisions and transfer the vibrational excitation energy back to kinetic energy.

8. EQUILIBRIUM ELECTRON FLUX

In Figure 8 we show the equilibrium electron fluxes as a function of electron energy resulting from the degradation of injected 1 keV primary electrons in CO gas with fractional ionization ranging from 0 to 10^{-1}. Although not highly visible on the logarithmic energy scale in the degradation spectra, many sharp spikes are displayed in the energy range 970–1000 eV, which are the result of the discrete nature of the excitation and ionization processes and are less prominent at high fractional ionizations. They have negligible effects on the overall energy deposition process and can be avoided by assuming a smooth energy distribution of the primary electrons. At energies higher than about 100 eV the degradation spectra reflect

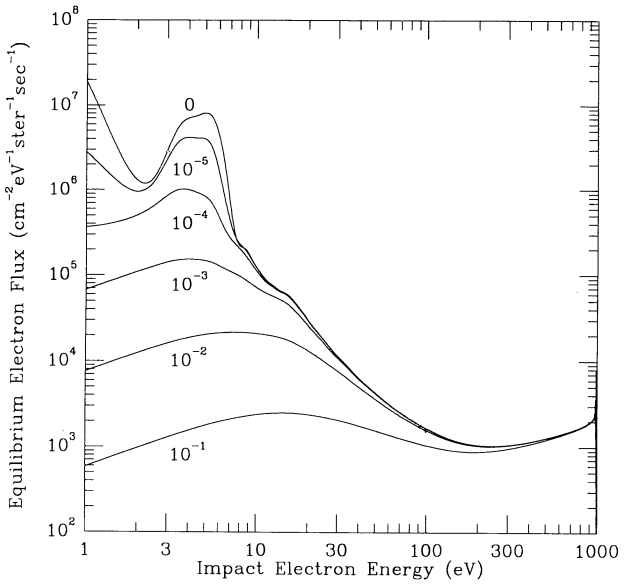

FIG. 8.—Electron degradation spectra of CO. The labels refer to the fractional ionization.

mainly the slowing down of the primary electrons. The rapid rise toward lower energies is the result of the distribution of the secondary electrons. The tip in the spectra located at 3–6 eV prominent for neutral and weakly ionized gas is the result of the small energy loss function by the only possible discrete process of vibrational excitation to the $v = 1$ level in that energy region. Also prominent for neutral and weakly ionized gas is the dip in the spectra located at 2–3 eV which is caused by the large energy loss function of the resonant vibrational excitation of CO. As the fractional ionization increases, both features are suppressed by the increasing importance of the energy loss to the ambient thermal electrons, and they disappear at fractional ionizations higher than 10^{-3}. The energy loss to heating increases and the electron flux decreases with increasing fractional ionization. The electron fluxes at lower energies decrease more than at higher energies because heating is more important at lower energies. As a result, the peak in the electron flux spectrum shifts to a higher energy as the fractional ionization rises. For highly ionized CO gas the effect of heating would be so prominent that the electron flux would be expected to decrease monotonically toward lower energies.

This work was supported by the National Science Foundation, Division of Astronomical Sciences, under grant AST-89-21939, and by the National Aeronautics and Space Administration, under grant NAGW-1561. We are grateful to J. M. Ajello, P. C. Cosby, A. Dalgarno, G. K. James, I. Kanik, L. A. Morgan, S. K. Srivastava, and S. Trajmar for discussions, and to A. Dalgarno for a careful reading of the manuscript.

REFERENCES

Aarts, J. F. M., & de Heer, F. J. 1970, J. Chem. Phys., 52, 5354
Ajello, J. M. 1971, J. Chem. Phys., 55, 3158
Allan, M. 1989, J. Electron. Spectrosc. Rel. Phenom., 48, 219
Boness, M. J. W., & Schulz, G. J. 1973, Phys. Rev. A, 8, 2883
Chung, S., & Lin, C. C. 1974, Phys. Rev. A, 9, 1954
Chutjian, A., & Tanaka, H. 1980, J. Phys. B, 13, 1901
Cooper, D. L., & Kirby, K. 1987, J. Chem. Phys., 87, 424
Cosby, P. C. 1993, J. Chem. Phys., 98, 7804
Cravens, T. E., Kozyra, J. U., Nagy, A. F., Gombosi, T. I., & Kurtz, M. 1987, J. Geophys. Res., 92, 7341
Cravens, T. E., Victor, G. A., & Dalgarno, A. 1975, Planet. Space. Sci., 23, 1059
Dalgarno, A., & Lejeune, G. 1971, Planet. Space Sci., 19, 1653
Ehrhardt, H., Langhans, L., Linder, F., & Taylor, H. S. 1968, Phys. Rev. A, 173, 222
Fox, J. L., & Dalgarno, A. 1979, Planet. Space Sci., 27, 491
Fox, J. L., Dalgarno, A., & Victor, G. A. 1977, Planet. Space Sci., 25, 71

Fox, J. L., & Taylor, H. A., Jr. 1990, Geophys. Res. Lett., 17, 1625
Fox, J. L., & Victor, G. A. 1988, Planet. Space Sci., 36, 329
Freund, R. S., Wetzel, R. C., & Shul, R. J. 1990, Phys. Rev. A, 41, 5861
Furlong, J., & Newell, W. R. 1993, in Proc. 18th Int. Conf. on Physics of Electronic and Atomic Collisions (abstr.) (Bristol: IOP)
Haddad, G. N., & Milloy, H. B. 1983, Australian J. Phys., 36, 473
Hake, R. D., & Phelps, A. V. 1967, Phys. Rev. A, 158, 70
Hille, E., & Märk, T. D. 1978, J. Chem. Phys., 69, 4600
Itikawa, Y., & Aono, O. 1966, Phys. Fluids, 9, 1259
Jain, D. K., & Khare, S. P. 1976, J. Phys. B, 9, 1429
James, G. K., Ajello, J. M., Kanik, I., Franklin, B., & Shemansky, D. E. 1992, J. Phys. B, 25, 1481
Kanik, I., Ratliff, M., & Trajmar, S. 1993a, Chem. Phys. Lett., 208, 341
Kanik, I., Trajmar, S., & Nickel, J. C. 1993b, J. Geophys. Res., 98, 7447
Kazansky, A. K., & Yelets, I. S. 1984, J. Phys. B, 17, 4767
Kirby, K., & Cooper, D. L. 1989, J. Chem. Phys., 90, 4895
Klots, C. E. 1968, in Fundamental Processes in Radiation Chemistry, ed. P. Ausloos (New York: Interscience), chap. 1, 40
Land, J. E. 1978, J. Appl. Phys., 49, 5716
Lee, M., & McKoy, V. 1982, J. Phys. B, 15, 3971
———. 1983, Phys. Rev. A, 28, 697
le Floch, A. 1991, Molec. Phys., 72, 133
Liu, W., Dalgarno, A., & Lepp, S. 1992, ApJ, 396, 679
Mason, N. J., & Newell, W. R. 1988, J. Phys. B, 21, 1293
Middleton, A. G., Brunger, M. J., & Teubner, P. J. O. 1992, J. Phys. B, 25, 3541
———. 1993, J. Phys. B, 26, 1743
Morgan, L. A. 1991, J. Phys. B, 4649
Morgan, L. A., & Tennyson, J. 1993, J. Phys. B, 26 2429
Mumma, M. J., Stone, E. J., & Zipf, E. C. 1971, J. Chem. Phys., 54, 2627
Opal, C. B., Peterson, W. K., & Beaty, E. C. 1971, J. Chem. Phys., 55, 4100
Orient, O. J., & Srivastava, S. K. 1987, J. Phys. B, 20, 3923
Potts, A. W., & Williams, T. A. 1974, J. Electron. Spectrosc. Rel. Phenom., 3, 3
Ransil, B. J. 1960, Rev. Mod. Phys., 32, 239
Rapp, D., & Englander-Golden, P. 1965, J. Chem. Phys., 43, 1464
Sawada, T., Sellin, D. L., & Green, A. E. S. 1972, J. Geophys. Res., 77, 4819
Schunk, R. W., & Hays, P. B. 1971, Planet. Space Sci., 19, 113
Skubenich, V. V. 1967, Opt. Spectrosc., 23, 540
Sohn, W., Kochem, K., Jung, K., Ehrhardt, H., & Chang, E. S. 1985, J. Phys. B, 18, 2049
Sun, Q., Winstead, C., & McKoy, V. 1992, Phys. Rev. A, 46, 6987
Swartz, W. E., Nisbet, J. S., & Green, A. E. S. 1971, J. Geophys. Res., 76, 8425
Tilford, S. G., & Simmons, J. D. 1972, J. Phys. Chem. Ref. Data, 1, 147
Viala, Y. P., Letzerter, C., Eidelsberg, M., & Rostas, F. 1988, A&A, 193, 265
Weatherford, C., & Huo, W. M. 1990, Phys. Rev. A, 41, 186
Weaver, H. A., Feldman, P. D., McPhate, J. B., A'Hearn, M. F., Arpigny, C., & Smith, T. E. 1994, ApJ, 422, 374
Well, W. C., Borst, W. L., & Zipf, E. C. 1973, Phys. Rev. A, 8, 2463
Woods, T. N., Feldman, P. D., & Dymond, K. F. 1987, A&A, 187, 380
Woods, T. N., Feldman, P. D., Dymond, K. F., & Sahnow, D. J. 1986, Nature, 324, 436
Zubek, M., & Szmytkowski, C. 1977, J. Phys. B, 10, L27